

Quench Detection for High-Temperature Superconductor Conductors using Acoustic Thermometry

M. Marchevsky, E. Hershkovitz, X. Wang, S. A. Gourlay and S. Prestemon

Abstract— Detecting local heat-dissipating zones in high-temperature superconductor (HTS) magnets is a challenging task due to slow propagation of such zones in HTS conductors. For long conductor lengths voltage-based methods may not provide a sufficient sensitivity or redundancy, and therefore non-voltage based detection alternatives are being sought. One of those is the recently proposed method of Eigen Frequency Thermometry (EFT), which is an active acoustic technique for a fast and non-intrusive detection of “hot spots”, utilizing temperature dependence of the conductor elastic moduli. In the present work, we demonstrate efficiency of EFT for detecting localized heating in a 1.2 m-long sample of REBCO tape immersed in liquid nitrogen, and benchmark sensitivity of the acoustic detection with respect to voltage, hot spot temperature, and power dissipation in the conductor. Modifying the original technique for differential mode of operation enables a much improved sensitivity, and adds a hot spot localization capability. Furthermore, we adapt this technique to subscale coils wound with REBCO CORC® conductor built in the framework of US Magnet Development Program. A successful thermal-based detection of dissipation onset at the critical current for a two-layer canted CORC® dipole assembly is discussed.

Index Terms—Acoustic sensors, temperature sensors, superconducting coils, high-temperature superconductors, quench detection.

I. INTRODUCTION

HIGH-temperature superconductors (HTS) are increasingly being used for various applications. A recent progress in pushing up the engineering current density above 500 A/mm² in REBCO [1] and Bi-2212-based HTS conductors [2] has created an opportunity for developing high-field magnets operating at temperatures above liquid helium and significantly expanded operational margin of such magnets towards higher fields [3]. A combination of large temperature margin and an increase of heat capacity with temperature yields high stability of HTS conductors. Conductor motion and impregnation material fracturing being major sources of quenching in conventional superconductor-based magnets are not likely to cause quenching in their HTS counterparts, as the enthalpy of the HTS conductor at 4.2 K is at least three orders of magnitude larger than that of a low-temperature superconductor [4]. Still,

formation of a resistive zone in HTS can be provoked, either by a local heat deposition from resistive splices or by a presence of a material defect that lowers critical current density. Depending upon cooling conditions, such zone may either become persistent, corresponding to the flux flow regime at temperatures below critical, or develop into a normal zone heated above the critical temperature. An expansion of the latter is impeded by the same factors that cause high conductor stability: normal zone propagation in HTS is 2-3 orders of magnitude slower than in conventional superconductors [5]-[8]. As a consequence, a significant local temperature rise would yield only a modest resistive voltage that is hard to detect in the noisy (inductive voltages, power supply ripple, etc.) magnet operating environment. Therefore, voltage-based quench detection systems developed for conventional superconducting magnets may lack enough sensitivity to prevent thermal damage in quenching HTS conductors. Various non-voltage quench detection and localization alternatives were proposed in the past, based on transient variation of stress [9-11], magnetic field [12]-[14], and acoustic emission [15]-[18]. More recently, techniques involving interferometry [19], Rayleigh [20]-[23] and Raman scattering [24] in optical fibers, and stray capacitance monitoring [25] specifically aimed at HTS applications were demonstrated. However, all those techniques detect hot spot indirectly: either through mechanical or electromagnetic manifestation, or by relying upon a temperature-dependent property of another body (optical fiber, liquid cryogen) thermally coupled to the quenching conductor. Here, we discuss a different kind of technique that utilizes conductor itself as a distributed temperature sensor. Our approach has advantages of being fast, non-invasive and adaptable to existing coils and magnet systems.

II. SETUP AND INSTRUMENTATION

A. Operational principle

Our technique is based upon active acoustic interrogation of the monitored body (in this case, an HTS conductor) with 2-20 μ s-long rectangular pulses emitted regularly at 10-100 ms intervals by a mechanically-coupled piezoelectric transducer. Each pulse “diffuses” away from the emitter while undergoing multiple scatterings by body boundaries and interfaces, yielding a 1-5 ms-long acoustic transient acquired by a receiver. Despite its complex shape, the transient waveform is uniquely defined by the geometry and elastic properties of the

This work was supported by the US Department of Energy under Contract # DE-AC02-05CH11231. (Corresponding author: Maxim Marchevsky.)

M. Marchevsky, E. Hershkovitz, X. Wang, S. A. Gourlay and S. Prestemon are with Lawrence Berkeley National Laboratory, Berkeley, CA 94720 USA (e-mail: mmartchevskii@lbl.gov)

probed volume. The elastic moduli exhibit temperature dependence on the order of -10^{-5} K^{-1} for most solids which affects sound velocity. Therefore the multiply-scattered wave accumulates an additional delay every time it passes through a “hot spot”. Such delay is detected by comparing the most recent transient to a stored reference acquired at the beginning of the experiment. In practice, we measure “time shift” Δt between the waveforms that maximizes their cross-correlation. Our approach is similar to the “coda wave interferometry” technique developed primarily for geophysics applications [26],[27]. Details of instrumentation, data processing, and demonstration of EFT-based quench detection for a 10-cm long HTS tape stack were given in [28]. Here, we modify and scale up this technique towards detecting quenches on a $\sim 1 \text{ m}$ length scale of a typical high-field coil, and extend its applicability to subscale coils wound with HTS CORC[®] cable.

B. Acoustic quench detection in HTS tape

In order to detect quenches acoustically in a long conductor, care must be taken with regard to a specific vibrational mode excited with pulsed excitation. It is because damping of acoustic waves can be prohibitively large for end-to-end propagation, unless a specific low-loss wave mode is chosen. For a tape such low-damping traveling modes are expected to be those comprised within its plane, as they interact the least with the supporting structure, and do not couple to the cryogen bath due to absence of shear vibrations in liquids. Using ANSYS software, we simulated a mechanical transient in the tape upon pulsed excitation by a square-shaped piezo-transducer bonded to it. Typical material and dimensional characteristics for piezo-ceramics material and REBCO HTS tape conductor, including its $50 \mu\text{m}$ thick stainless substrate, and copper stabilizer layers of $30 \mu\text{m}$ -thickness at the REBCO side and $20 \mu\text{m}$ -thick at the back side were used for this simulation. The result is illustrated in Fig. 1 showing how a transversely-polarized piezo-plate excites the in-plane traveling wave mode in the tape. Upon a voltage pulse the piezo deforms not just transversely along the electric field direction, but also longitudinally, according to its Poisson ratio. The longitudinal deformation couples to the tape, reverberating and propagating towards its opposite end. Next, the experiment was conducted using a $\sim 1.2 \text{ m}$ long, 4 mm wide REBCO tape (Superpower, type SCS4050), placed on a 3 mm -thick flat G10 strip substrate,

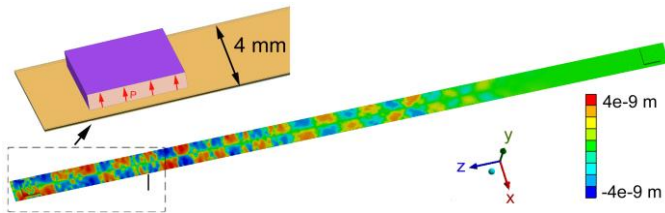


Fig. 1. Simulated in-plane transient wave propagating in a tape upon a pulsed 1 V p-p and $0.2 \mu\text{s}$ in duration excitation applied using a square-shaped piezoelectric transducer attached to the tape surface. Pulse is applied at $t_0 = 0.2 \mu\text{s}$; the directional deformation map with respect to x -axis at $t_1 = 20.6 \mu\text{s}$ is shown. Inset: magnified view of the tape and transducer geometry used in our simulation.

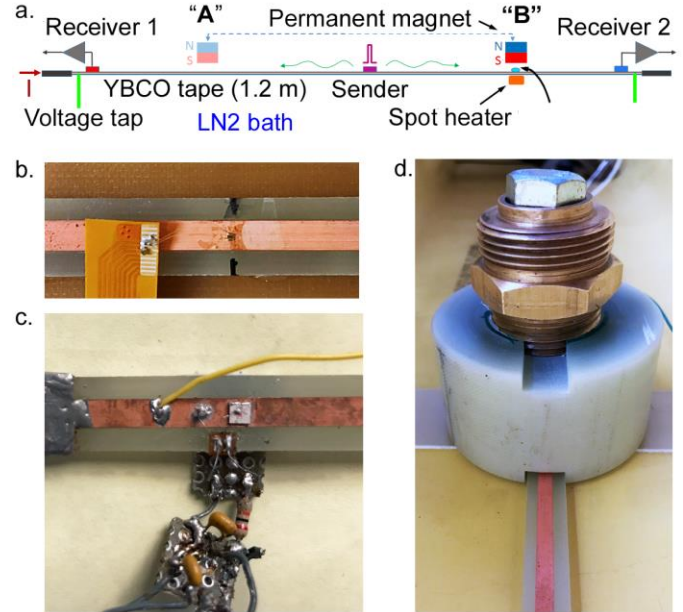


Fig. 2. (a) Sketch of the experimental setup (side view). (b) Cernox thermometer installed at the tape surface. (c) Piezo-transducer, a voltage tap, and a cryogenic preamplifier mounted on a breadboard. (d) Permanent magnet in assembly set atop of the tape surface.

soldered at the ends to copper tape-based current leads, and instrumented with two voltage taps separated by 1120 mm distance (Fig. 2a). Two square-shaped $3.0 \times 3.0 \times 0.55 \text{ mm}$ piezoelectric transducers (receivers) polarized across thickness (Steminc, Inc., type SM410) were installed 1080 mm apart at each end of the REBCO tape using Indium solder. Custom-built cryogenic preamplifiers with gain 10 in a $0\text{-}1 \text{ MHz}$ bandwidth were assembled on breadboards and mounted next to the piezo-transducers. A third (sender) transducer of same type was installed in the middle of the tape, at 523 mm distance from sensor “1” and 557 mm from sensor “2”. A Cernox thermometer (Lakeshore, CX-1050BR) was mounted at the REBCO side of the tape using insulating varnish (Lakeshore, VGE-7031) at the location “B”, 310 mm from the sender transducer and 247 mm from sensor “2”. The thermometer differential sensitivity at 77 K is $-2.412 \Omega/\text{K}$, per manufacturer’s

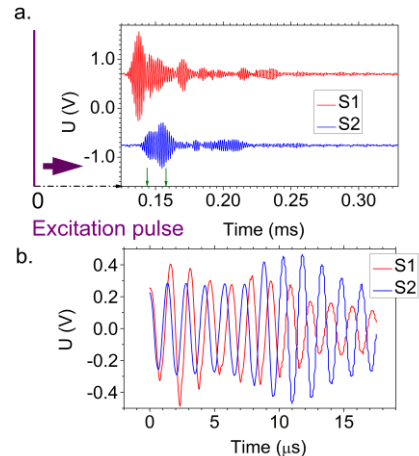


Fig. 3. (a) Transient waveforms acquired by the receiver transducers installed at the tape ends (offset vertically for clarity). (b) Sub-waveforms selected from the transients for quench monitoring.

specifications. A spot heater made of $6.3 \times 3.2 \times 0.6$ mm-sized SMD type metal film resistor of 5.3Ω was affixed with varnish on the opposite side of the tape, directly underneath the thermometer. We used a cylindrically-shaped SmCo permanent magnet of 25 mm in diameter to create a reversible local depression of tape critical current. The magnet was installed inside a mechanical assembly that allowed its re-positioning along the tape, while maintaining a vertical clearance gap. For the majority of current ramps the magnet assembly was placed in location “B” (see Fig. 2a), right above the thermometer. Magnet vertical position was adjusted to create ~ 0.3 T field at the tape surface. The entire setup was placed in an open horizontal foam cryostat filled with liquid nitrogen, having the tape completely submerged at ~ 20 mm depth. Lambda 6 V / 200 A power supply was used to apply current to the tape in 1 A steps, and Keysight 34420A nanovoltmeter to monitor tape voltage. For the acoustic measurements, Keysight 33600A waveform generator and PicoScope4000a USB scope were used, in combination with custom-developed LabView DAQ and processing software. Acoustic waveforms were acquired at 40 MHz sampling rate.

In the first current up-ramp with no magnet in place the tape end-to-end critical current was found to be 95 A using $1 \mu\text{V}/\text{cm}$ voltage criterion. The n -value calculated from the current-voltage characteristic was 34. Current was ramped up to 107 A, yielding maximal voltage across the tape of 19.75 mV. With magnet placed in location “A”, critical current dropped to 54 A, while n -value decreased to 16. Current was ramped up to 66 A yielding tape voltage of 7.8 mV. With magnet in location “B”, critical current was 56.8 A, and $n = 14$. Current was ramped up to 75 A, yielding tape voltage of 7.6 mV. All current-voltage characteristics were consistent, with no sign of conductor degradation upon multiple transitions through the critical current. For the duration of each current ramp, we applied rectangular pulses of $2 \mu\text{s}$ width, 10 V p-p in amplitude to the sender transducer at 10 Hz rate. Transient acoustic waves then propagated towards tape ends, and were monitored by the receiver transducers. In Fig. 3 the resulting waveforms are shown; the time interval between the pulse emission and wave arrival to the sensor “1” was $128.2 \mu\text{s}$, while for the sensor “2” it was $138.2 \mu\text{s}$, yielding mean sound velocity in the tape of ~ 4050 m/s. Since the out-of-plane traveling wave is damped by the spot heater resistor bonded to the tape; the initial portion of the transient acquired by sensor “2” is lower in amplitude. For the quench detection purpose we focus on monitoring a later arriving portion of the transient, same for both sensors, in the interval marked with arrows in Fig. 3a plot and shown separately in Fig. 3b. The result of simultaneous monitoring of tape voltage, temperature and acoustic transient time shift for the current ramp with permanent magnet positioned at “B” are shown in Fig. 4, indicating a correlation between acoustic and voltage signals as tape goes resistive due to the permanent magnet locally suppressing its critical current. For the acoustic signals, we plot the *sum*: $\Delta t_{S1} + \Delta t_{S2}$ and the *difference*: $\Delta t_{S1} - \Delta t_{S2}$ of the individual time shifts. Measuring the latter, *differential* time shift allows for an efficient suppression of various common mode

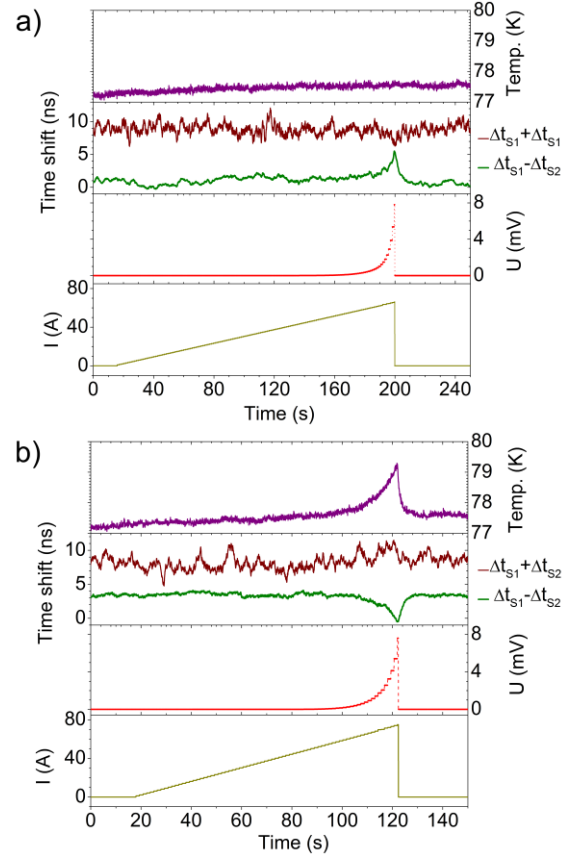


Fig. 4. (a) Results of quench detection experiment with magnet in location “A”. (b) Results of quench detection experiment with magnet in location “B”.

noise sources, and eliminates spurious signals due to thermal fluctuations of the entire tape, as evident comparing the difference and sum signals. Sensitivity to local hot spots in differential mode is thus significantly improved compared to the original one sender / one receiver detection scheme used in [28]. As heating should increase Δt for the corresponding tape segment, sign of the differential signal is indicative of whether sensor “1” or sensor “2” adjacent tape side is quenching. For magnet location “A”, the change in differential acoustic signal is $+5.5$ ns (with Signal to Noise Ratio of ~ 2.2), measured at $1.22 I_c$ and peak conductor dissipation power of 0.51 W. For magnet location “B”, the signal change is -3.5 ns (SNR ~ 2.7) at $1.32 I_c$ and peak dissipation power of 0.57 W. Assuming the hot spot is constrained with the magnet diameter, the latter number translates to a local heat flux towards nitrogen bath of $2850 \text{ W}/\text{m}^2$. The thermometer mounted at location “B” allows for a direct thermal cross-calibration. The measured peak hot

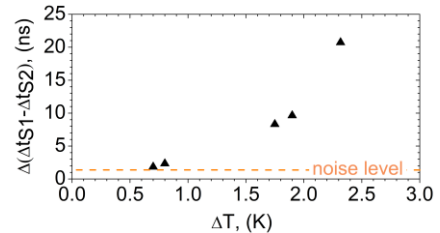


Fig. 5. Variation of the differential time shift as function of temperature upon firing the spot heater.

spot temperature is only ~ 1.6 K above the background at the maximal applied current, which is consistent with nucleate boiling regime of liquid nitrogen [29] at the calculated heat flux condition. To further calibrate our system, we performed five heater firing experiments with no transport current in the tape, and the magnet being removed. Heater voltages were 4.0, 4.6, 4.8, 5 and 6 V; heater was kept on until temperature and acoustic signal equilibrated, typically for 5-8 s. The measured variation of $\Delta t_{S1} - \Delta t_{S2}$ versus variation of tape temperature are plotted in Fig. 5. Thermal contribution to the acoustic time shift is clearly distinguishable above the noise background for $\Delta T > 0.7$ K. We therefore conclude that local thermal sensitivity of better than 1 K is readily achievable with our technique for detecting hot spots in a bare ~ 1 m long REBCO tape immersed in liquid nitrogen. It should be noted, that the linear conductor geometry and its direct contact with cryogenic liquid create the most challenging combination of conditions for the thermal-based acoustic detection. In magnet windings where the conductor is epoxy-impregnated, its cooling is less efficient, and a higher hot spot temperature is expected which would be easier to detect. Also, acoustic waves can travel across windings turn-to-turn rather than along the conductor, thus reducing the required sender-receiver distance and further improving the sensitivity.

C. Quench detection in CORC[®] dipole coil assembly

We adapted our technique to detect quenching in the prototype two-layer dipole assembly wound with HTS CORC[®] [30] cable. The coil assembly layers are wound in ‘‘Canted Cosine Theta’’ [31] pattern around the 3D-printed ‘‘blue stone’’ mandrels using CORC[®] conductor comprising 29 REBCO tapes (2 mm wide and 30 μm -thick substrate) distributed around a copper core wire of 2.56 mm diameter. The cable diameter is 3.63 mm, and its full length in each layer is 2.25 m, including out-of-mandrel portions. Layers are spliced in series using Indium-filled and bolt-tightened copper block. Details of the CCT CORC[®] coil development can be found in [32, 33]. The coil is instrumented with voltage taps and custom-built acoustic transducers (Fig. 6a), having two sender transducer of same configuration mounted at the coil terminals facing the splice block, and two receiver transducers mounted at the outer terminals of each coil (Fig. 6b). The receiver transducers were combined with MOSFET cryogenic preamplifiers [17]. Experiments were conducted in liquid nitrogen. Pulses of 80 V p-p amplitude and 13.2 μs in duration were applied to the sender transducers at 10 Hz rate. It was found that two distinct propagating waves coexist in the CORC[®] cable: one is likely asso-

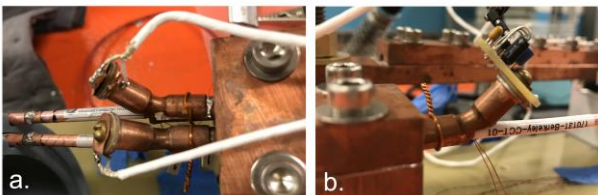


Fig. 6. (a) Custom-built sender transducers mounted near the coil splice block. (b) Receiver transducer with integrated cryogenic amplifier mounted at the coil lead end.

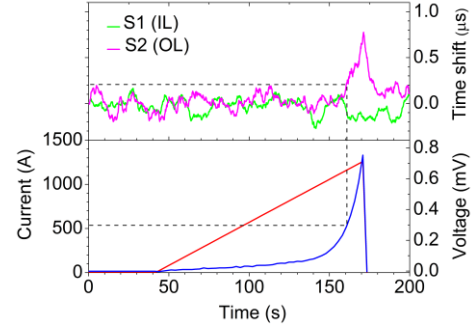


Fig. 7. (a) Acoustic time shift acquired by sensors installed at the lead end of the inner and outer coil layers. (b) Current and voltage in the coil, plotted as function of time.

ciated with the solid copper core, and another one with propagation along the HTS tapes. The former wave appears to be more robust, and it travels faster, thus being associated with the initial portion of the transient waveform acquired by the sensors. We therefore selected that portion of the transient for quench detection monitoring. Results of the experiment are summarized in Fig. 7, showing coil current, voltage and time shift acquired for the two layers as function of time. The acoustic time shift rises above background noise level at $I = 537$ A which corresponds to the coil voltage of 0.3 mV and power dissipation of 0.16 W in the cable. Based on the individual layer voltage data, the outer layer starts transitioning first, at a lower current, yielding net heat over the full current ramp of 3.7 J, while the inner layer heat is 3.08 J. However, the time shift variation at the transition was only detected for the outer layer. This could be due to a weaker coupling between the transducers and the inner layer cable, or an additional acoustic damping caused by the mechanical contact between the inner layer cable and the outer layer mandrel. Further experiments, as well as transducer re-design for improved mechanical coupling are in progress.

III. CONCLUSIONS

We used the novel non-voltage acoustic technique for real-time monitoring of localized hot spots with better than 1 K thermal sensitivity, and demonstrated detection of quenches in longer than 1 m-long bare REBCO conductors and coils wound with REBCO tape-based CORC[®] cable. By measuring differential time shift of the acoustic transients, local sensitivity of the detection and its redundancy with respect to ambient thermal background has been greatly improved, also adding localization capability. Being non-invasive, the technique may be useful in situations where placing voltage taps is difficult or prohibitive, and improve redundancy and reduce operational risks for the existing magnet systems. Future potential of the technique using multiple sensor arrays applied to various styles of HTS subscales is currently under investigation.

ACKNOWLEDGMENT

Authors are thankful to M. Reynolds and H. Higley for the mechanical and cryogenic support, and to M. Turqueti and J. Taylor for assistance with the CORC[®] coil testing.

REFERENCES

- [1] K. Tsuchiya, A. Kikuchi, A. Terashima, K. Norimoto, M. Uchida, M. Tawada, M. Masuzawa, N. Ohuchi, X. Wang, T. Takao, S. Fujita, "Critical current measurement of commercial REBCO conductors at 4.2 K", *Cryogenics*, vol. 85, pp. 1-7, 2017. [Online] Available: <https://doi.org/10.1016/j.cryogenics.2017.05.002>.
- [2] D. C. Larbalestier, J. Jiang, U. P. Trociewitz, F. Kametani, C. Scheuerlein, M. Dalban-Canassy, M. Matras, P. Chen, N. C. Craig, P. J. Lee, and E. E. Hellstrom, "Isotropic round-wire multifilament cuprate superconductor for generation of magnetic fields above 30 T", *Nature Materials* vol. 13, pp. 375–381, 2014. [Online] Available: <http://dx.doi.org/10.1038/nmat3887>
- [3] E. Todesco, L. Bottura, G. De Rijk, L. Rossi, "Dipoles for High-Energy LHC", *IEEE Trans. Appl. Supercond.*, vol. 24, 4004306, 2014. [Online] Available: <http://dx.doi.org/10.1109/TASC.2013.2286002>
- [4] Y. Iwasa, "Case Studies in Superconducting Magnets", ISBN: 978-0-306-44881-2. [Online] Available: <https://link.springer.com/book/10.1007/b115039>
- [5] F. Trillaud, H. Palanki, U. Trociewitz, S. Thompson, H. Weijers, and J. Schwartz, "Normal zone propagation experiments on HTS composite conductors," *Cryogenics*, vol. 43, no. 3, pp. 271–279, 2003. [Online]. Available: <http://www.sciencedirect.com/science/article/pii/S0011227503000444>
- [6] X. Wang, A. R. Caruso, M. Breschi, G. Zhang, U. P. Trociewitz, H. W. Weijers, and J. Schwartz, "Normal zone initiation and propagation in Y-Ba-Cu-O coated conductors with Cu stabilizer," *IEEE Trans. Appl. Supercond.*, vol. 15, pp. 2586–2589, 2005. [Online] Available: <http://dx.doi.org/10.1109/TASC.2005.847661>
- [7] H. H. Song and J. Schwartz, "Stability and Quench Behavior of YBa₂Cu₃O_{7-x} Coated Conductor at 4.2 K, Self-Field," *IEEE Trans. Appl. Supercond.*, vol. 19, pp. 3735–3743, 2009. [Online] Available: <http://dx.doi.org/10.1109/TASC.2009.2023674>
- [8] J. van Nugteren, "Normal Zone Propagation in a YBCO Superconducting Tape" MSc Thesis, Univ. of Twente, 2012.
- [9] N. Tamada, F. Schauer, and Y. Iwasa, "A stress detection technique for stressed structures, including superconducting magnets," *Appl. Phys. Lett.* vol. 41, pp. 36–38, 1982. [Online] Available: <http://dx.doi.org/10.1063/1.93313>
- [10] A. Ninomiya, K. Sakaniwa, H. Kado, T. Ishigohka, and Y. Higo, "Quench detection of superconducting magnets using ultrasonic wave," *IEEE Trans. Magn.*, vol. 25, pp. 1520–1523, 1989. [Online] Available: <http://dx.doi.org/10.1109/20.92585>
- [11] T. Ishigohka, O. Tsukamoto, and Y. Iwasa, "Method to detect a temperature rise in superconducting coils with piezoelectric sensors," *Appl. Phys. Lett.*, vol. 43, no. 3, pp. 317–318, 1983. [Online]. Available: <http://dx.doi.org/10.1063/1.94298>
- [12] D. Leroy, J. Krzywinski, V. Remondino, L. Walckiers, and R. Wolf, "Quench observation in LHC superconducting one meter long dipole models by field perturbation measurements," *IEEE Trans. Appl. Supercond.*, vol. 3, pp. 781–784, 1993. [Online] Available: <http://dx.doi.org/10.1109/77.233820>
- [13] T. Ogitsu, A. Devred, K. Kim, J. Krzywinski, P. Radusewicz, R. I. Schermer, T. Kobayashi, K. Tsuchiya, J. Muratore, and P. Wanderer, "Quench antenna for superconducting particle accelerator magnets," *IEEE Trans. Magn.*, vol. 30, pp. 2273–2276, 1994. [Online] Available: <http://dx.doi.org/10.1109/20.305728>
- [14] M. Marchevsky, J. DiMarco, H. Felice, A. R. Hafalia, J. Joseph, J. Lizarazo, X. Wang, and G. Sabbi, "Magnetic detection of quenches in high-field accelerator magnets," *IEEE Trans. Appl. Supercond.* vol. 23, pp. 9001005 - 9001005, 2013. [Online] Available: <http://dx.doi.org/10.1109/TASC.2012.2236379>
- [15] O. Tsukamoto, J. F. Maguire, E. S. Bobrov, and Y. Iwasa, "Identification of quench origins in a superconductor with acoustic emission and voltage measurements," *Appl. Phys. Lett.* vol. 39, p. 172-174, 1981. [Online] Available: <http://dx.doi.org/10.1063/1.92652>
- [16] H. Lee, Ho Min Kim, J. Jankowski, and Y. Iwasa, "Detection of 'Hot Spots' in HTS Coils and Test Samples With Acoustic Emission Signals," *IEEE Trans. Appl. Supercond.* 14, 1298, 2004. [Online] Available: <http://dx.doi.org/10.1109/TASC.2004.830559>
- [17] M. Marchevsky, G. Sabbi, H. Bajas, and S. Gourlay, "Acoustic emission during quench training of superconducting accelerator magnets," *Cryogenics*, v. 69, pp. 50–57, 2015. [Online] Available: <http://dx.doi.org/10.1016/j.cryogenics.2015.03.005>
- [18] M. Yoneda, N. Nanato, D. Aoki, T. Kato, and S. Murase, "Quench detection/protection of an HTS coil by AE signals," *Physica C: Superconductivity and its Applications*, the 23rd International Symposium on Superconductivity, vol. 471, no. 21, pp. 1432 – 1435, 2011. [Online]. Available: <http://www.sciencedirect.com/science/article/pii/S0921453411002978>
- [19] J. M. van Oort, R. M. Scanlan, and H. H. J. ten Kate, "A fiber-optic strain measurement and quench localization system for use in superconducting accelerator dipole magnets," *IEEE Trans. Appl. Supercond.*, vol. 5, pp. 882–885, 1995. [Online] Available: <http://dx.doi.org/10.1109/77.402689>
- [20] W. K. Chan, G. Flanagan, and J. Schwartz, "Spatial and temporal resolution requirements for quench detection in (RE)Ba₂Cu₃O_x magnets using Rayleigh-scattering-based fiber optic distributed sensing," *Supercond. Sci. Technol.*, vol. 26 p. 105015, 2013. [Online]. Available: <http://dx.doi.org/10.1088/0953-2048/26/10/105015>
- [21] F. Scurti, S. Ishmael, G. Flanagan, and J. Schwartz, "Quench detection for high temperature superconductor magnets: a novel technique based on Rayleigh-backscattering interrogated optical fibers," *Supercond. Sci. Technol.*, vol. 29, no. 3, p. 03LT01, 2016. [Online]. Available: <http://dx.doi.org/10.1088/0953-2048/29/3/03LT01>
- [22] F. Scurti, S. Sathyamurthy, M. Rupich and J. Schwartz, "Self-monitoring "SMART" (RE)Ba₂Cu₃O_{7-x} conductor via integrated optical fibers", *Supercond. Sci. Technol.* in press. 2017. [Online] Available: <https://doi.org/10.1088/1361-6668/aa8762>
- [23] F. Scurti and J. Schwartz, "Optical fiber distributed sensing for high temperature superconductor magnets," 2017 25th Optical Fiber Sensors Conference (OFS), Jeju, 2017. pp. 1-4, doi: 10.1117/12.2265947
- [24] Z. Amira, M. Bouyahi, T. Ezzedine, "Measurement of Temperature through Raman Scattering," *Procedia Computer Science*, vol. 73, 2015, pp. 350-357, 2015. [Online] Available: <http://dx.doi.org/10.1016/j.procs.2015.12.003>
- [25] E. Ravaioli, M. Marchevsky, G. L. Sabbi, T. Shen, and K. Zhang, "Quench Detection Utilizing Stray Capacitances," preprint EUCAS2017 Conference, 3LP4-23; *IEEE Trans. Appl. Supercond.* 2017. [Online] Available: doi: 10.1109/TASC.2018.2812909
- [26] R. Snieder, "The Theory of Coda Wave Interferometry", *Pure Appl. Geophys.*, vol. 163, pp. 455–473, 2006. [Online] Available: <https://doi.org/10.1007/s00024-005-0026-6>
- [27] R. L. Weaver and O. I. Lobkis, "Temperature dependence of diffuse field phase", *Ultrasonics*, vol. 38, pp. 491–494, 2000. [Online] Available: [https://doi.org/10.1016/S0041-624X\(99\)00047-5](https://doi.org/10.1016/S0041-624X(99)00047-5)
- [28] M. Marchevsky and S. A. Gourlay, "Acoustic thermometry for detecting quenches in superconducting coils and conductor stacks," *Appl. Phys. Lett.*, vol. 110, p. 012601, 2017. [Online]. Available: <http://dx.doi.org/10.1063/1.4973466>
- [29] T. M. Flynn, J. W. Draper, and J. J. Roos, "The Nucleate and Film Boiling Curve of Liquid Nitrogen at One Atmosphere," *Adv. Cryogen. Eng.* vol. 7 pp. 539-545, 1962. [Online] Available: <http://dx.doi.org/10.1007/978-1-4757-0531-7>
- [30] J. D. Weiss, T. Mulder, H. J. ten Kate, and D. C. van der Laan, "Introduction of CORC® wires: highly flexible, round high-temperature superconducting wires for magnet and power transmission applications," *Supercond. Sci. Technol.*, vol. 30, p. 014002, 2016. [Online] Available: <http://dx.doi.org/10.1088/0953-2048/30/1/014002>
- [31] S. Caspi, F. Borgnolutti, L. Brouwer, D. Cheng, D. R. Dietderich, H. Felice, A. Godeke, R. Hafalia, M. Martchevskii, S. Prestemon, E. Rochepault, C. Swenson, and X. Wang, "Canted-Cosine-Theta Magnet (CCT)—A Concept for High Field Accelerator Magnets," *IEEE Trans. Appl. Supercond.*, vol. 24, pp. 1-4, 2014. [Online] Available: <http://dx.doi.org/10.1109/TASC.2013.2284722>
- [32] S. Gourlay, A. Zlobin, S. Prestemon, D. Larbalestier, and L. Cooley, "US Magnet Development Program Plan" 2016. [Online] Available: <https://doi.org/10.13140/RG.2.2.34915.14883>
- [33] X. Wang, S. Caspi, D. R. Dietderich, W. B. Ghiorso, S. A. Gourlay, H. C. Higley, A. Lin, S. O. Prestemon, D. van der Laan and J. D. Weiss, "A viable dipole magnet concept with REBCO CORC® wires and further development needs for high-field magnet applications", *Supercond. Sci. Technol.*, vol. 31, pp. 045007, 2018. [Online] Available: <https://doi.org/10.1088/1361-6668/aaad8f>